

An Open-Source Frequency-Domain Model for Floating Wind Turbine Design Optimization

Matthew Hall, Stein Housner, Daniel Zalkind, Pietro Bortolotti,
David Ogden, Garrett Barter

National Renewable Energy Laboratory
15013 Denver West Parkway, Golden, CO, USA

E-mail: matthew.hall@nrel.gov

Abstract. A new frequency-domain dynamics model has been developed that uses open-source components to efficiently represent a complete floating wind turbine system. The model, called RAFT (Response Amplitudes of Floating Turbines), incorporates quasi-static mooring reactions, strip-theory and potential-flow hydrodynamics, blade-element-momentum aerodynamics, and linear turbine control. The formulation is compatible with a wide variety of support structure configurations and no manual or time-domain preprocessing steps are required, making RAFT very practical in design and optimization workflows. The model is applied to three reference floating wind turbine designs and its predictions are compared with results from time-domain OpenFAST simulations. There is good agreement in mean offsets as well the statistics and spectra of the dynamic response, verifying RAFT's general suitability for floating wind analysis. Follow-on work will include verification of potential-flow and turbine-control features and application to optimization problems.

1. Introduction

Frequency-domain models are an important tool for designing floating structures because they can calculate a system's coupled response orders of magnitude more quickly than time-domain simulations. They work by constructing a linear, frequency-dependent representation of the system and then solving for the harmonic, steady-state system response at each excitation frequency. Such approaches have long been used in floating structure design, and were first adapted to model floating wind turbines by adding the turbine's effects in their most simplified form as constant stiffness, damping, and added mass terms (e.g., [1, 2]). More recent approaches have accounted for frequency dependencies in the aerodynamics as well [3, 4, 5].

Most frequency-domain floating wind turbine models to date have been oriented toward support structure optimization, relying on separate time-domain preprocessing of the turbine properties—a computational expense that only needs to be incurred once if the turbine design does not change. However, research efforts are increasingly focusing on *control co-design*, wherein integrated optimization of the support structure, turbine, and controller can offer significant design improvements compared to designing each portion sequentially. This design paradigm calls for all parts of the system to be modeled efficiently in the frequency domain, including the aerodynamics and control (e.g., [4]).

This paper presents a new model, dubbed RAFT (Response Amplitudes of Floating Turbines), that was created as part of the WEIS (Wind Energy with Integrated Servo-controls)



Toolset [6] to meet the specific needs of control co-design optimization with high computational efficiency. RAFT incorporates quasi-static mooring reactions, strip-theory and potential-flow hydrodynamics, blade-element-momentum aerodynamics, and linear turbine control in a way that avoids any time-domain preprocessing. The design parameterization supports a wide range of substructure geometries, and it is open source to promote further expansion and broad usability. The following sections detail RAFT's modeling approach and initial verification findings, in which its outputs are compared with results from OpenFAST for three different reference designs.

2. Modeling Approach

As a frequency-domain model, RAFT is based on a linear, frequency-dependent equation for the floating system's steady-state response. In other words, the excitation and response are assumed to be stationary (nonvarying frequency content). External forces are represented as a mean force, $\bar{\mathbf{f}}$, plus a Fourier series of complex amplitudes, $\hat{\mathbf{f}}(\omega)$, which represent both amplitude and phase at each frequency, ω . The system is assumed linear such that responses to each excitation frequency are harmonic and can be superimposed. The system response is then a summation of the mean response, $\bar{\boldsymbol{\xi}}$, and a Fourier series of complex response amplitudes, $\hat{\boldsymbol{\xi}}(\omega)$.

The system's dynamic response as a function of frequency is solved from the following frequency-dependent equation of motion, which shows the different terms considered by RAFT:

$$(-\omega^2[\mathbf{M}_{struc} + \mathbf{A}_{sub}(\omega) + \mathbf{A}_{aero}(\omega)] + i\omega[\mathbf{B}_{sub}(\omega) + \mathbf{B}_{aero}(\omega)] + \mathbf{C}_{struc} + \mathbf{C}_{moor})\hat{\boldsymbol{\xi}}(\omega) = \hat{\mathbf{f}}(\omega). \quad (1)$$

The matrix \mathbf{M} is the floating structure's mass and inertia, \mathbf{A} is added mass, \mathbf{B} is damping, \mathbf{C} is stiffness, and $\hat{\mathbf{f}}(\omega)$ is excitation from wind or waves. The matrix subscripts are discussed in later sections. Not shown in (1) is that some of the coefficients represent linearizations of inherently nonlinear phenomena, creating a nonlinear dependence on $\hat{\boldsymbol{\xi}}(\omega)$. This is handled in RAFT using an iterative solution process.

The frequency-domain dynamics described by (1) are assumed to act about an operating point defined as the system's mean state for a given load case. The mean position is found by solving the static equilibrium equation:

$$\mathbf{C}_{struc} \bar{\boldsymbol{\xi}} = \bar{\mathbf{f}}_{aero} + \bar{\mathbf{f}}_{hydro} + \bar{\mathbf{f}}_{moor}(\bar{\boldsymbol{\xi}}), \quad (2)$$

where \mathbf{C}_{struc} is the total hydrostatic stiffness matrix, $\bar{\mathbf{f}}_{aero} + \bar{\mathbf{f}}_{hydro}$ is the mean wind and wave load, and $\bar{\mathbf{f}}_{moor}(\bar{\boldsymbol{\xi}})$ is the nonlinear mooring system reaction force (which includes the effective mooring stiffness).

In the above equations, RAFT considers six rigid-body degrees of freedom for the floating platform; surge, sway, heave, roll, pitch, and yaw make up the six elements of the response vector $\boldsymbol{\xi}$. When modeling turbine control, an additional degree of freedom for rotor speed variations is solved for using a separate set of equations described in Section 2.5.

2.1. Design Parameterization

RAFT parameterizes a floating wind turbine design by representing the substructure as a combination of cylindrical or rectangular members, the tower as a tapered cylindrical member, the nacelle as a lumped mass, and the rotor blades as a series of blade elements (Figure 1).

The members that make up the substructure are defined along axes going between any two locations in the structure. Mirroring the geometry parameterization in WEIS [6], members have diameter d (or side lengths $sl^{(1)}$ and $sl^{(2)}$ for rectangular members) and wall-thickness t at user-specified station points along their length. Linear transitions between stations allow for tapered sections, and any ballast quantity and density can be specified in these sections. End caps and

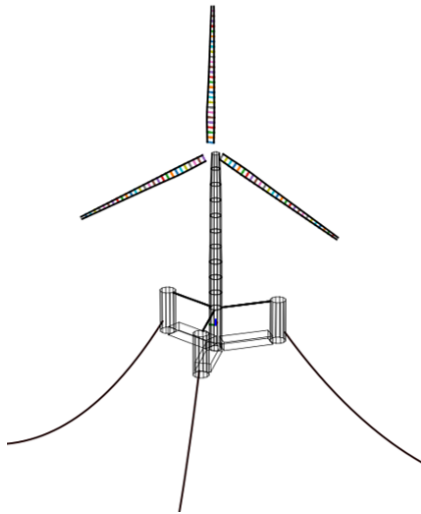


Figure 1: Example of RAFT's member-based parameterization

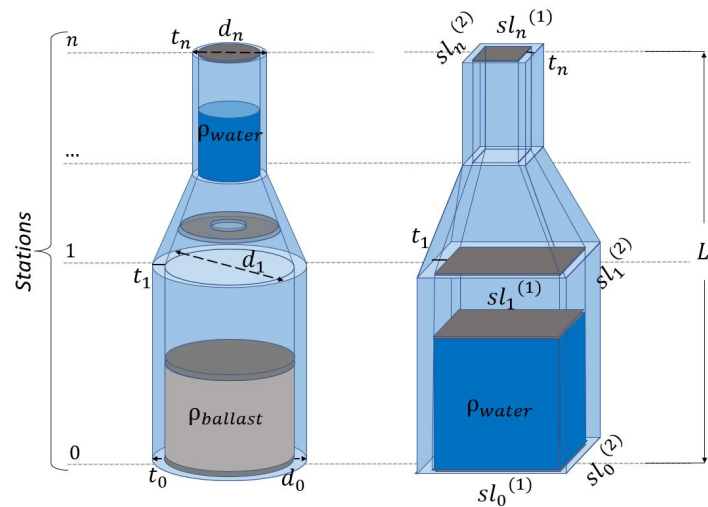


Figure 2: Example circular and rectangular members featuring tapered sections, ballast, and bulkheads

bulkheads can also be added at any location along the member length. Figure 2 illustrates example member geometries. A member can also hold its own hydrodynamic added mass and drag coefficients, along with a discretization length used to subdivide the member into strips for hydrodynamic calculations. The wind turbine tower is represented as a single cylindrical member with any number of sections and tapers, as well as wall thickness variations.

The rotor-nacelle assembly has different aerodynamic and structural representations. Aerodynamically, it is represented by three identical rotor blades with dimensions and lift-drag polar properties distributed at user-specified station points along the length. Structurally, the rotor-nacelle assembly is represented as a single lumped-parameter body that provides for mass and inertia coefficients as well as an offset location from the tower centerline. The turbine control system is described by a schedule of target rotor speeds, blade pitch angles, and controller gains as a function of wind speed.

Combining these elements gives a complete floating wind turbine design description (Figure 1) that can be recorded using input files that follow the YAML format given in the RAFT GitHub repository [7].

RAFT takes an object-oriented approach with the various parts of the floating wind system, using generic functions to interact with each component and transform motions, forces, and coefficient matrices between different reference frames. Currently, these approaches use small angle assumptions and neglect nonlinear terms such as centripetal, Coriolis, and gyroscopic effects, but there is potential to linearize these in future work. Further details are omitted here for brevity.

2.2. Mass and Hydrostatics

RAFT computes the floating structure's mass and hydrostatic properties by summing the contributions of all the members in the floating platform as well as the tower and the rotor-nacelle assembly.

A local six-by-six mass and inertia matrix is calculated for each member, based on the distributed masses of its structural shell, ballast, end caps, and bulkheads. These matrices are then transformed to be about the platform reference point—the point on the platform where the tower centerline intersects the still water line—and added to a total system mass matrix,

\mathbf{M}_{struc} . The total structure center of mass is also tracked during this process.

A similar process is carried out to get the total displaced volume and hydrostatic stiffness properties of the structure. The hydrostatic stiffness matrix (not accounting for weight) of any member relative to the platform reference point is

$$\mathbf{K}_{hydro,i} = \begin{bmatrix} 0 & 0 & 0 & 0 & 0 & 0 \\ 0 & 0 & 0 & 0 & 0 & 0 \\ 0 & 0 & \rho g A_{wp} & \rho g A_{wp} y_{wp} & -\rho g A_{wp} x_{wp} & 0 \\ 0 & 0 & \rho g A_{wp} y_{wp} & \rho g I_{xx} + \rho g V z_{cb} & -\rho g A_{wp} x_{wp} y_{wp} & 0 \\ 0 & 0 & -\rho g A_{wp} x_{wp} & -\rho g A_{wp} x_{wp} y_{wp} & \rho g I_{yy} + \rho g V z_{cb} & 0 \\ 0 & 0 & 0 & 0 & 0 & 0 \end{bmatrix}. \quad (3)$$

where A_{wp} is water plane area, x_{wp} and y_{wp} are the coordinates of the water plane, V is the displaced volume, and z_{cb} is the vertical center-of-volume location. I_{xx} and I_{yy} are the water plane area moments of inertia about the x and y directions, respectively. This matrix is computed for each member about the platform reference point, then summed to obtain the total system hydrostatic stiffness matrix. The equations in (3) also apply to fully submerged members by zeroing the water plane area ($A_{wp} = 0$). Members fully out of the water, such as the tower, are excluded. Contributions from structure weight to the hydrostatic stiffness are also included in the pitch and roll directions according to $-m_{total}g z_{cg}$, resulting in the total floating structure stiffness matrix \mathbf{C}_{struc} of (1).

2.3. Mooring System and Mean Offsets

The mooring system in RAFT is modeled using MoorPy, a quasi-static mooring system model that also includes floating bodies with linear hydrostatic properties [8]. RAFT passes the mooring system description to MoorPy, sets up a floating body with identical hydrostatic properties as the floating wind turbine (\mathbf{C}_{struc}), and specifies applied loads on the body equal to the total mean applied load on the floating system. MoorPy then solves for equilibrium of this system, which is equivalent to solving (2), and returns the mean offsets $\bar{\xi}$ along with the mean mooring reaction force $\bar{\mathbf{f}}_{moor}(\bar{\xi})$, the mooring system stiffness about the offset location \mathbf{C}_{moor} , the individual mooring line tensions, and a Jacobian of mooring line tension with respect to each platform degree of freedom. These latter two quantities are used by RAFT to estimate mooring line tension dynamics.

2.4. Hydrodynamics

The default hydrodynamics model in RAFT is a strip-theory approach that applies the relative form of the Morison equation to all submerged members. Additionally, RAFT can use linear hydrodynamic coefficients from the potential flow solver HAMS [9]. For this purpose, RAFT has built-in meshing routines for the substructure geometry and calls HAMS through a Python-based wrapper so that the hydrodynamic preprocessing happens automatically. This capability will be covered in future work.

The strip-theory hydrodynamics approach is based on the relative form of the Morison equation for transverse flow across a strip of a cylinder, which accounts for both wave velocity, u , and body velocity, v :

$$\Delta f = \left[\underbrace{\rho(1 + C_a) \frac{\pi}{4} D^2 \dot{u}}_{inertia} - \underbrace{\rho C_a \frac{\pi}{4} D^2 \dot{v}}_{added\ mass} + \underbrace{\frac{1}{2} \rho C_d D (u - v) |u - v|}_{drag} \right] \Delta l, \quad (4)$$

where Δf is hydrodynamic force, D is cylinder diameter, Δl is strip length, C_a is the added mass coefficient, and C_d is the drag coefficient. In RAFT, each term in (4) is adapted for

different directions and, in the case of rectangular members, for different area and volume calculations as shown in equations (5-7). Each member is discretized into strips to which the equations are applied based on the local geometry and wave kinematics. Wave-induced water velocity, acceleration, and dynamic pressure amplitudes are computed at the center of each strip according to Airy wave equations for intermediate water depth.

For each strip, a local added mass matrix, \mathbf{A}_L , is calculated based on the strip's volume and orientation:

$$\mathbf{A}_L = \rho \Delta V (C_{a,p1} \mathbf{p}_1 \mathbf{p}_1^T + C_{a,p2} \mathbf{p}_2 \mathbf{p}_2^T), \quad (5)$$

where \mathbf{p}_1 and \mathbf{p}_2 are the orthogonal transverse unit vectors and $C_{a,p1}$ and $C_{a,p2}$ are the corresponding added mass coefficients, which can be different in the case of rectangular cross sections. The added mass matrices of all strips are transformed to the platform reference point and summed to get the overall substructure added mass matrix \mathbf{A}_{sub} .

Inertial excitation forces are calculated using the same factors along with the local fluid acceleration at the node as a function of wave frequency, $i\omega \hat{\mathbf{u}}_L(\omega)$:

$$\hat{\mathbf{f}}_{I,L}(\omega) = \rho \Delta V [(1 + C_{a,p1}) \mathbf{p}_1 \mathbf{p}_1^T + (1 + C_{a,p2}) \mathbf{p}_2 \mathbf{p}_2^T] i\omega \hat{\mathbf{u}}_L(\omega). \quad (6)$$

Axial terms are also supported. They follow a similar approach as the transverse terms but calculate the effective volume based on a hemisphere sized according to the strip's axial exposed area. This area is also used to calculate axial dynamic pressure loads.

RAFT linearizes the quadratic drag term in Morison's equation by approximating it as a damping term with coefficient $\sqrt{8/\pi} \sigma_u C_d$, where σ_u is the standard deviation of the relative water velocity [10]. A local damping matrix is set up for each strip and has the form

$$\mathbf{B}_L = \frac{1}{2} \rho \sqrt{\frac{8}{\pi}} (\sigma_{u,q} A_q C_{d,q} \mathbf{q} \mathbf{q}^T + \sigma_{u,p1} A_{p1} C_{d,p1} \mathbf{p}_1 \mathbf{p}_1^T + \sigma_{u,p2} A_{p2} C_{d,p2} \mathbf{p}_2 \mathbf{p}_2^T), \quad (7)$$

where A_q is the effective axial drag area of the strip, $C_{d,q}$ is the specified axial drag coefficient, and \mathbf{q} is the axial unit vector. As with added mass, the local damping matrices of the member nodes are transformed to the platform reference point and summed to get the overall substructure damping matrix, \mathbf{B}_{sub} . The drag contribution to excitation forces is obtained by applying the local water velocity amplitudes

$$\hat{\mathbf{f}}_{d,L}(\omega) = \mathbf{B}_L \hat{\mathbf{u}}_L(\omega) \quad (8)$$

and then translating these complex frequency-dependent force amplitude vectors back to the platform reference point and summing.

2.5. Rotor Aerodynamics and Control

RAFT incorporates wind turbine aerodynamics and control modeling to efficiently solve for the coupled floating wind turbine dynamic response without requiring manual aerodynamic preprocessing steps. The rotor aerodynamics at each mean wind speed of interest are modeled in CCBlade, a steady-state blade-element-momentum theory solver [11]. RAFT provides CCBlade with the distributed blade properties and the wind speed, wind shear, rotor speed, and blade pitch angle for the current load case. CCBlade computes the steady-state rotor power and torque, along with their derivatives with respect to blade pitch angle, wind speed, and rotor speed. These outputs are azimuthally averaged. The steady-state quantities are used in calculating annual energy production and mean system loads, while their derivatives are used in computing aerodynamic contributions to system dynamics.

When wind turbine control is disabled, RAFT assumes the rotor speed and blade pitch angle are constant. The affect of rotor aerodynamics on the dynamic response is modeled using the derivative of thrust with respect to wind speed, denoted T_U , which provides the damping

coefficient for fore-aft nacelle motion and can be multiplied by the rotor-averaged hub-height wind speed spectrum to provide the aerodynamic excitation force amplitudes as a function of frequency. Both the damping and excitation terms are then transformed based on the hub height to account for the effects on platform surge and pitch motions, resulting in the final aerodynamic excitation vector, $\hat{\mathbf{f}}_{\text{aero}}(\omega)$, and damping matrix, $\mathbf{B}_{\text{aero}}(\omega)$.

When control is included, RAFT considers fluctuations in rotor speed, $\Omega(\omega)$, and blade pitch, $\beta(\omega)$, to model rotor aerodynamic contributions to aerodynamic added mass, damping, and excitation. These contributions are derived using linearized equations of motion for the rotor thrust and speed dynamics, expanding on the work of Souza et al. [12] to also include generator torque control, turbulent wind excitation, and nacelle-velocity feedback control.

Rotor thrust, T , can be linearized and expressed in the time domain as

$$T = \bar{T} + T_U \Delta(U - \dot{x}) + T_\Omega \Delta\Omega + T_\beta \Delta\beta, \quad (9)$$

where U is the rotor-averaged wind speed, \dot{x} is the fore-aft nacelle velocity, and subscripts of T denote partial derivatives of thrust with respect to the subscripted variables. A similar linearization can be done for generator torque, Q , which can then be used to form the following equation for generator speed dynamics:

$$I_r \dot{\Omega} = Q_U \Delta(U - \dot{x}) + Q_\Omega \Delta\Omega + Q_\beta \Delta\beta - N_g \Delta\tau_g, \quad (10)$$

where I_r is the rotor's mass moment of inertia, N_g is the gearbox ratio, and τ_g is the generator torque.

What remains to be defined in equations (9) and (10) are the blade-pitch and generator torque control inputs, $\Delta\beta$ and $\Delta\tau_g$. The blade-pitch control term includes proportional and integral gains ($k_{P\beta}$ and $k_{I\beta}$) along with a nacelle-velocity-feedback gain, k_{Px} to help damp platform motions [13]:

$$\Delta\beta = k_{P\beta} \Delta\Omega + k_{I\beta} \int \Delta\Omega dt + k_{Px} \dot{x}. \quad (11)$$

The generator torque control term includes proportional and integral gains:

$$\Delta\tau_g = k_{p,\tau} \Delta\Omega + k_{I,\tau} \int \Delta\Omega dt. \quad (12)$$

The above equations are combined in the frequency domain to give the following equation for frequency-dependent variations in rotor thrust:

$$T(\omega) = T_U U(\omega) - (T_U - k_{Px} T_\beta) i\omega x(\omega) - H_{QT}(\omega) [Q_U U(\omega) - (Q_U - k_{Px} Q_\beta) i\omega x(\omega)], \quad (13)$$

where $H_{QT}(\omega)$ is the transfer function from rotor torque to thrust:

$$H_{QT}(\omega) = \frac{(T_\Omega + k_{P\beta} T_\beta) i\omega + k_{I\beta} T_\beta}{\omega^2 I_r + i\omega(Q_\Omega + k_{P\beta} Q_\beta - N_g k_{P\tau}) + k_{I\beta} Q_\beta - N_g k_{I\tau}}. \quad (14)$$

From this, the fore-aft terms for aerodynamic added mass, damping, and turbulent wind excitation can be extracted:

$$a_{\text{aero}}(\omega) = \Re \left\{ \frac{1}{i\omega} [T_U - k_{Px} T_\beta - H_{QT}(\omega) (Q_U - k_{Px} Q_\beta)] \right\}, \quad (15)$$

$$b_{\text{aero}}(\omega) = \Re [T_U - k_{Px} T_\beta - H_{QT}(\omega) (Q_U - k_{Px} Q_\beta)], \quad (16)$$

$$\hat{\mathbf{f}}_{\text{aero}}(\omega) = (T_U - H_{QT}(\omega) Q_U) U(\omega) = H_{Uf}(\omega) U(\omega). \quad (17)$$

These hub-height quantities are then transformed to be about the platform reference point, accounting for their coupled affect on surge and pitch in the final aerodynamic added mass matrix, $\mathbf{A}_{\text{aero}}(\omega)$, damping matrix, $\mathbf{B}_{\text{aero}}(\omega)$, and excitation vector, $\hat{\mathbf{f}}_{\text{aero}}(\omega)$.

2.6. Solution Process

The coefficient calculations described above for the various modeling aspects that go into Eq. (1) are evaluated at different times in RAFT's execution. An overview of the sequence is as follows:

- Evaluate structure mass and hydrostatic characteristics
- Model mooring system and solve unloaded equilibrium position
- Evaluate linear hydrodynamic coefficients, including excitation at select sea states
- Evaluate aerodynamic coefficients at select wind speeds
- Apply mean loads and solve for mean offset position
- Reevaluate aerodynamic coefficients to account for tilt
- Compute rotor response coefficients (including effect of control)
- Linearize viscous drag excitation and damping at given sea state
- Solve for system response
- Iterate over previous three steps until response convergence

Because the wind and waves are assumed uncorrelated, RAFT computes the system responses to wave excitation and wind excitation independently, then sums the resulting power spectral densities.

3. Verification Results

To demonstrate and verify RAFT, models have been set up for three reference designs: the OC3 Hywind spar [14], the OC4-DeepCwind semisubmersible [15], and the VoltturnUS-S semisubmersible [16]. These models were analyzed in terms of static properties, mean offsets, natural frequencies, and dynamic responses under a stochastic sea state and steady wind—in all cases comparing the results against either reference values or results from equivalent OpenFAST simulations. Rotor aerodynamic coefficients calculated for the IEA 15-MW Reference Turbine [17] including the effect of control are also shown for demonstration.

3.1. Model Setup

The wind turbine and mooring system properties were set up in RAFT based on the reference input files for these designs. For the substructure, a more manual approach was taken because RAFT's geometry parameterization has some differences with those of OpenFAST and WISDEM. The substructure properties were therefore tuned manually to match the published reference design properties [14, 15, 16]. The most challenging properties to match were the mass distribution and the hydrodynamic coefficients. RAFT models the mass based on the description of each member, meaning that specific member properties (wall thickness, ballast levels, etc.) had to be reverse engineered to meet the overall mass properties of the reference designs. For hydrodynamics, only the strip-theory capability in RAFT was used for the present work. As such, the drag and added mass coefficients for the members had to be tuned carefully to match the overall hydrodynamic properties. This was especially important for the VoltturnUS-S design, for which distributed drag and added mass coefficients are not yet defined or published.

The OpenFAST models were run using the standard publicly available model input files for each of the three reference designs, including turbine structural degrees of freedom to provide a representative comparison with how OpenFAST typically models a floating turbine.

3.2. Static Properties

Table 1 shows percent differences between RAFT model calculations and the reference values for select static properties of the three designs. Most static properties such as mass and stiffness coefficients agree with reference specifications to within 1%.

Table 1: Comparison of static properties from reference and RAFT values

| | OC3-Hywind | | OC4-DeepCwind | | VolturnUS-S | |
|---|------------|---------|---------------|----------|-------------|----------|
| | Ref | RAFT | Ref | RAFT | Ref | RAFT |
| Turbine Tower Mass (t) | 249.7 | 249.6 | 249.7 | 249.6 | 1,263.0 | 1,249.9 |
| Turbine Tower z_{cg} (m) | 43.40 | 43.35 | 43.40 | 43.35 | 56.5 | 56.01 |
| Substructure Mass (t) | 7,466.3 | 7,476.1 | 13,473.0 | 13,685.4 | 17,854.0 | 17,806.5 |
| Substructure z_{cg} (m) | -89.92 | -89.89 | -13.46 | -13.46 | -14.94 | -15.25 |
| Roll/Pitch Inertia (10^6 kg-m ²) | 64,329 | 64,062 | 9,267 | 9,126 | 16,495 | 16,132 |
| Buoyancy Force (kN) | 80,708 | 80,735 | 139,890 | 139,959 | 203,176 | 198,932 |
| C_{33} (kN/m) | 332 | 333 | 3,836 | 3,822 | 4,470 | 4,491 |
| C_{44} and C_{55} (MN-m/rad) | -4,999 | -5010 | -377 | -383 | 2,190 | 2,299 |

3.3. Mean Responses to Steady Load

Figure 3 shows each of the three floating systems modeled by RAFT in their undisplaced positions and in their displaced positions under a steady 11.5-m/s wind and no waves. Table 2 gives the mean platform offsets, upwind mooring line tensions, and tower-base bending moments calculated from OpenFAST results and predicted by RAFT in this condition.

Table 2: Comparison of mean responses to 11.5 m/s wind from OpenFAST and RAFT

| | OC3-Hywind | | OC4-DeepCwind | | VolturnUS-S | |
|-------------------|------------|-------|---------------|-------|-------------|-------|
| | OpenFAST | RAFT | OpenFAST | RAFT | OpenFAST | RAFT |
| Surge (m) | 11.1 | 11.0 | 4.9 | 4.8 | 15.5 | 13.9 |
| Heave (m) | -0.17 | -1.12 | -0.02 | -0.22 | -0.09 | -1.43 |
| Pitch (deg) | 2.57 | 2.70 | 1.85 | 1.88 | 2.46 | 3.63 |
| T_{moor} (kN) | 1171 | 1247 | 1002 | 1033 | 3531 | 3792 |
| M_{base} (MN-m) | 44.8 | 29.7 | 40.3 | 24.6 | 203.6 | 219.2 |

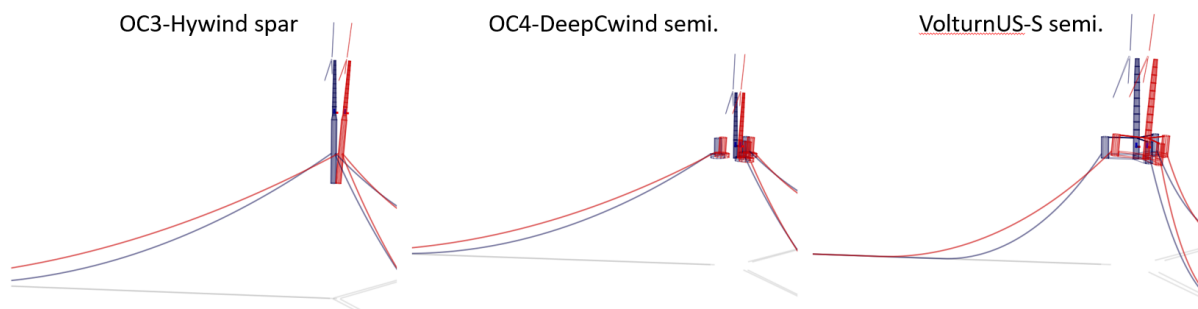


Figure 3: RAFT models in undisplaced (blue) and displaced (red) positions at 11.5 m/s wind

3.4. Natural Frequencies

RAFT computes the stiffness and inertia matrices from which the system natural frequencies and mode shapes can be solved. The natural periods calculated by RAFT for the three designs

are compared with the reference values in Table 3. Differences in yaw natural periods arose from difficulties in matching the yaw inertias during reverse engineering of the designs.

Table 3: Comparison of natural periods (s) from OpenFAST and RAFT

| | OC3 | | OC4 | | VolturnUS-S | |
|-------|-------|-------|-------|-------|-------------|-------|
| | Ref | RAFT | Ref | RAFT | Ref | RAFT |
| Surge | 123.5 | 120.5 | 111.1 | 105.5 | 142.9 | 121.2 |
| Sway | 123.5 | 120.5 | 111.1 | 105.5 | 142.9 | 120.9 |
| Heave | 30.4 | 30.8 | 17.2 | 17.3 | 20.4 | 19.7 |
| Roll | 31.5 | 29.5 | 25.0 | 25.0 | 27.8 | 26.2 |
| Pitch | 31.5 | 29.5 | 25.0 | 25.0 | 27.8 | 26.2 |
| Yaw | 8.2 | 6.5 | 76.9 | 75.0 | 90.9 | 76.9 |

3.5. Aerodynamic Coefficients

RAFT's modeling of the turbine aerodynamics and control is linear, meaning that the turbine's affects on the floating system can be represented as a set of added mass, damping, and excitation coefficients. These coefficients are frequency-dependent and also depend on the turbine's control settings and the mean wind speed. To illustrate, Figure 4 shows the rotor aerodynamic added mass, damping, and excitation coefficients calculated for the IEA 15-MW Reference Turbine. These coefficients use the blade-pitch and generator-torque control settings included with the UMaine VolturnUS-S reference design. Three wind speeds are below rated and three are above rated, showing the large affect of wind speed on the coefficients. The figure also shows corresponding rotor-averaged wind speed amplitudes calculated for the turbine's rotor area with class IB turbulence levels.

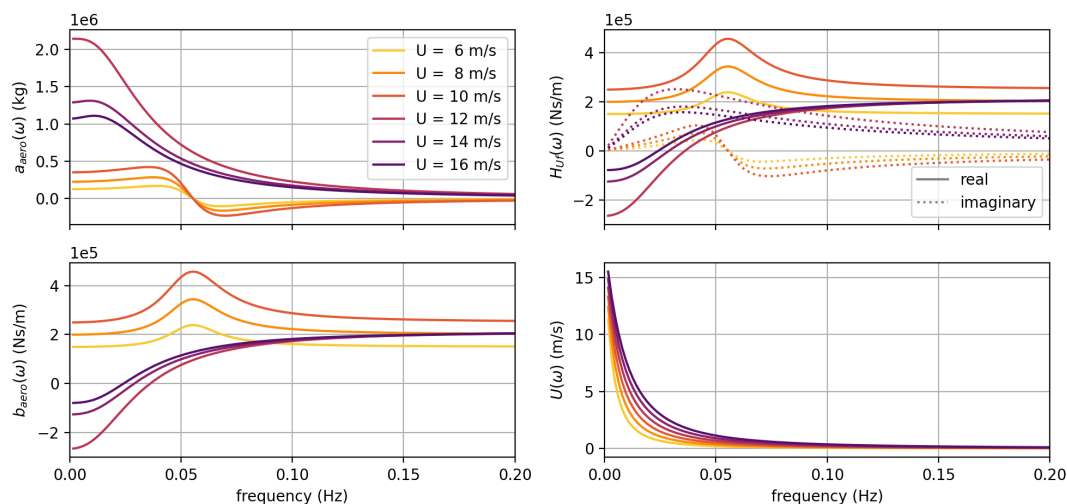


Figure 4: Calculated aerodynamic added mass, damping, and excitation coefficients and rotor-averaged wind speed amplitudes for the IEA 15-MW Reference Turbine over six wind speeds

3.6. Dynamic Response

Figure 5 shows the power spectral densities from RAFT and OpenFAST simulations of the three designs under steady 8-m/s winds and irregular waves (JONSWAP spectrum with 12-s peak period and 6-m significant wave height). RAFT matches the overall platform response characteristics predicted by OpenFAST fairly well. The two most notable differences are that RAFT overpredicts the OC4-DeepCwind semisubmersible heave response at 0.06 Hz, and that RAFT's prediction of the VoltturnUS-S pitch response is more spread out, with a lower peak but extending into lower frequency ranges than those predicted by OpenFAST.

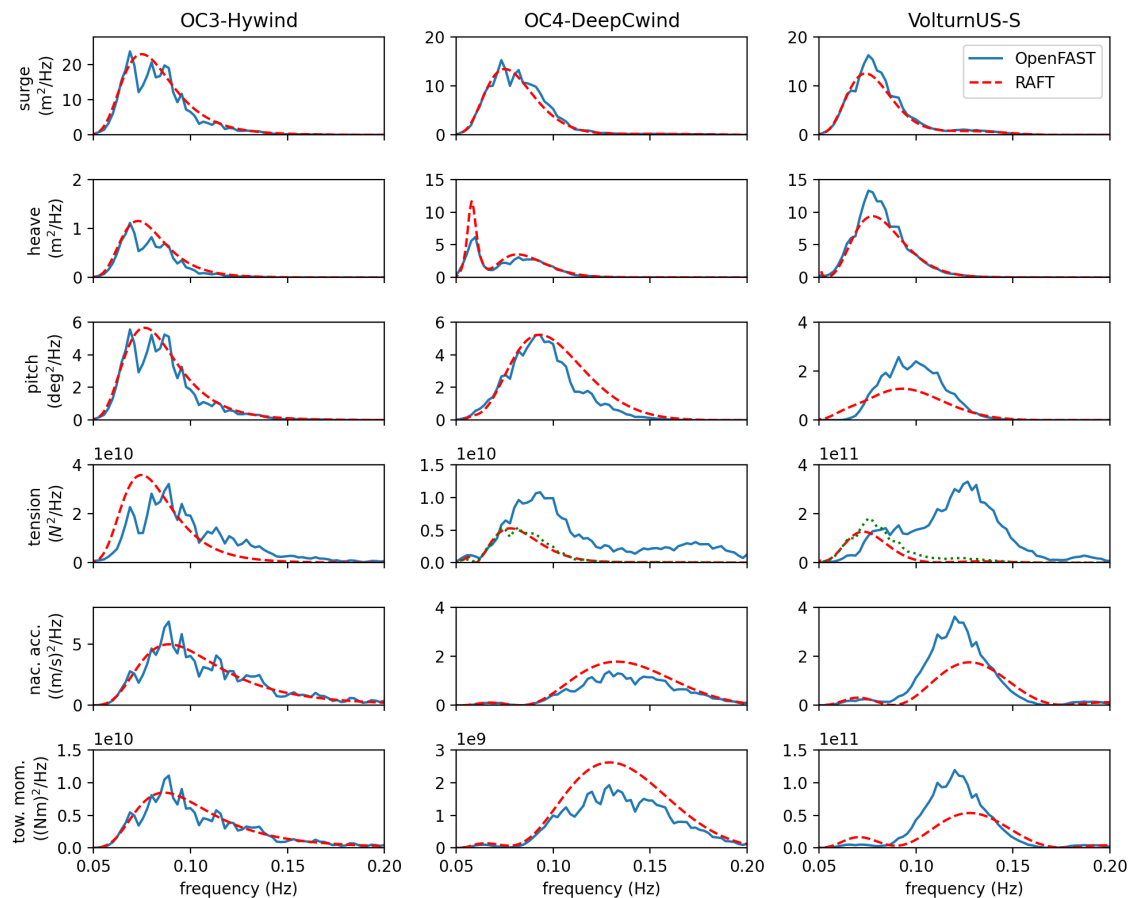


Figure 5: Power spectral densities of response to irregular waves and steady wind

The differences seem to be largest where diffraction and radiation effects would be greatest, suggesting that they are caused by RAFT's reliance on strip-theory hydrodynamics for these results, neglecting the potential-flow hydrodynamic phenomena that would be represented in OpenFAST. In the case of the OC4-DeepCwind semisubmersible, the platform's large heave plates would interact most with the free surface in the vertical direction and at the lowest frequencies, which is where the greatest platform motion difference is seen. Similarly, the VoltturnUS-S semisubmersible's large rectangular pontoons could have significant interaction with the free surface, especially at lower frequencies. The pontoons could experience heave and pitch excitation from transverse dynamic pressure loads, which are not currently modeled in RAFT due to the slender-member strip-theory assumptions. These pontoons would also cause significant wave-radiation damping, which is not captured in RAFT's strip theory approach. These modeling differences could explain the differences seen in the VoltturnUS-S design's heave

and pitch responses. These hypotheses will be explored in follow-on work that will incorporate potential-flow hydrodynamic inputs from HAMS into the RAFT analyses.

The largest differences in Figure 5 are in the upwind mooring line fairlead tensions. RAFT predicts significantly lower values for the two semisubmersible designs above 0.08 Hz. This is well explained by RAFT's use of a linearized quasi-static mooring model, which neglects the drag and inertia effects that become significant at higher platform motion frequencies. When OpenFAST is run with a quasi-static model, the tensions agree very well with RAFT's predictions. This is demonstrated by the dotted green lines shown for the OC4-DeepCwind and VoltturnUS-S designs' mooring tensions in Figure 5, which are predicted by OpenFAST when using its quasi-static mooring model.

Differences in RAFT's prediction of nacelle acceleration and tower-base fore-aft bending moment (which accounts for both applied force and inertial effects) are consistent with the differences observed in platform motions.

From the calculated response spectra, RAFT estimates standard deviations from which extreme values can also be estimated. Table 4 compares the standard deviations corresponding to the cases shown in Figure 5. These statistics show good agreement in platform response, underprediction of mooring tensions, and good agreement in tower-base bending moment considering the modeling approximations involved.

Table 4: Standard deviation comparison

| | OC3-Hywind | | OC4-DeepCwind | | VoltturnUS-S | |
|-------------------|------------|------|---------------|------|--------------|------|
| | OpenFAST | RAFT | OpenFAST | RAFT | OpenFAST | RAFT |
| Surge (m) | 0.9 | 0.9 | 0.7 | 0.7 | 0.7 | 0.6 |
| Heave (m) | 0.16 | 0.19 | 0.39 | 0.43 | 0.59 | 0.56 |
| Pitch (deg) | 0.43 | 0.47 | 0.47 | 0.50 | 0.31 | 0.25 |
| T_{moor} (kN) | 14 | 9 | 25 | 13 | 129 | 59 |
| M_{base} (MN-m) | 21.6 | 22.1 | 10.7 | 13.1 | 63.5 | 53.3 |

4. Conclusions

A new frequency-domain model for floating wind turbines, RAFT, has been developed and tested with three reference designs in comparison to OpenFAST results. These tests checked the model's handling of static properties, floating system offsets under steady wind loads, and coupled dynamic response. The dynamic results accounted for strip-theory hydrodynamics, linearized quasi-static mooring dynamics, and linearized aerodynamics. The model predictions show good levels of agreement with OpenFAST results considering the fidelity level, with disagreement levels usually less than 10% in platform motions and tower-base loads. Larger disagreements were noted in the mooring tension response and the VoltturnUS-S platform's pitch response. These are attributed to the lack of mooring dynamic effects and potential-flow hydrodynamics. Future work will incorporate these factors, as well as control terms, to further improve the model. Nevertheless, the model achieves its primary goal of providing an integrated, open-source, and automated means of quickly evaluating floating wind turbine designs.

Acknowledgments

This work was authored by the National Renewable Energy Laboratory, operated by Alliance for Sustainable Energy, LLC, for the U.S. Department of Energy (DOE) under Contract No. DE-AC36-08GO28308. Funding provided by the DOE ARPA-E ATLANTIS program under a

2020 project titled, “WEIS: A Tool Set to Enable Controls Co-Design of Floating Offshore Wind Energy Systems.” The views expressed in the article do not necessarily represent the views of the DOE or the U.S. Government. The U.S. Government retains and the publisher, by accepting the article for publication, acknowledges that the U.S. Government retains a nonexclusive, paid-up, irrevocable, worldwide license to publish or reproduce the published form of this work, or allow others to do so, for U.S. Government purposes.

References

- [1] E. Wayman, *Coupled Dynamics and Economic Analysis of Floating Wind Turbine Systems*. Masters thesis, MIT, May 2006.
- [2] M. Hall, B. Buckham, and C. Crawford, “Evolving offshore wind: Genetic Algorithm-Based optimization of floating wind turbine platforms,” in *MTS/IEEE Oceans’13*, June 2013.
- [3] A. M. Pegalajar-Jurado, M. Borg, and H. Bredmose, “An efficient frequency-domain model for quick load analysis of floating offshore wind turbines,” *Wind Energy Sci.*, vol. 3, 2018.
- [4] R. C. Lupton and R. S. Langley, “Improved linearised models of wind turbine aerodynamics and control system dynamics using harmonic linearisation,” *Renew. Energy*, vol. 135, 2019.
- [5] J. M. Hegseth, E. E. Bachynski, and J. R. R. A. Martins, “Integrated design optimization of spar floating wind turbines,” *Marine Structures*, vol. 72, July 2020.
- [6] J. Jonkman, A. Wright, G. Barter, M. Hall, J. Allison, and D. R. Herber, “Functional requirements for the WEIS toolset to enable controls Co-Design of floating offshore wind turbines,” in *ASME 3rd International Offshore Wind Technical Conference*, 2020.
- [7] NREL, “RAFT version 1.0,” 2021. <https://github.com/WISDEM/RAFT>.
- [8] M. Hall, S. Housner, S. Srinivas, and S. Wilson, “MoorPy: quasi-static mooring analysis in python,” 2021. <https://www.osti.gov/biblio/1810090>.
- [9] Y. Liu, “HAMS: a Frequency-Domain preprocessor for wave-structure interactions,” *Journal of Marine Science and Engineering*, vol. 7, Mar. 2019.
- [10] L. E. Borgman, “Random hydrodynamic forces on objects,” *The Annals of Mathematical Statistics*, vol. 38, no. 1, p. 37–51, 1967.
- [11] S. A. Ning, “A simple solution method for the blade element momentum equations with guaranteed convergence,” *Wind Energy*, vol. 17, no. 9, 2014.
- [12] C. E. S. Souza, J. M. Hegseth, and E. E. Bachynski, “Frequency-Dependent aerodynamic damping and inertia in linearized dynamic analysis of floating wind turbines,” *Journal of Physics: Conference Series*, vol. 1452, Jan. 2020.
- [13] N. J. Abbas, D. S. Zalkind, L. Pao, and A. Wright, “A reference open-source controller for fixed and floating offshore wind turbines,” *Wind Energy Science*, vol. 7, no. 1, 2022.
- [14] J. M. Jonkman, “Definition of the floating system for phase IV of OC3,” Tech. Rep. NREL/TP-5000-47535, National Renewable Energy Laboratory, Golden, Colorado, 2010.
- [15] A. Robertson, J. Jonkman, M. Masciola, H. Song, A. Goupee, A. Coulling, and C. Luan, “Definition of the semisubmersible floating system for phase II of OC4,” Tech. Rep. NREL/TP-5000-60601, 1155123, National Renewable Energy Laboratory, Sept. 2014.
- [16] C. Allen, A. Viselli, H. Dagher, A. Goupee, E. Gaertner, N. Abbas, M. Hall, and G. Barter, “Definition of the UMaine VoltturnUS-S reference platform developed for the IEA wind 15-Megawatt offshore reference wind turbine,” Tech. Rep. NREL/TP-5000-76773, 2020.
- [17] E. Gaertner, J. Rinker, L. Sethuraman, F. Zahle, B. Anderson, G. E. Barter, N. J. Abbas, F. Meng, P. Bortolotti, W. Skrzypinski, G. N. Scott, R. Feil, H. Bredmose, K. Dykes, M. Shields, C. Allen, and A. Viselli, “IEA Wind TCP Task 37: Definition of the IEA 15-Megawatt Offshore Reference Wind Turbine,” Tech. Rep. NREL/TP-5000-75698, National Renewable Energy Laboratory, 2020.